



Coexistence of Multiple Attractors and Crisis Route to Chaos in a Novel Chaotic Jerk Circuit

J. Kengne*, Z. T. Njitacke*,†, A. Nguomkam Negou*,†,
M. Fouodji Tsostop*† and H. B. Fotsin*,†

*Laboratoire d'Automatique et Informatique Appliquée (LAIA),
Department of Electrical Engineering, IUT-FV Bandjoun,
University of Dschang, Cameroon

†Laboratory of Electronics and Signal Processing,
Department of Physics, University of Dschang,
P.O. Box 67, Dschang, Cameroon

Received September 18, 2015; Revised November 12, 2015

In this paper, a novel autonomous RC chaotic jerk circuit is introduced and the corresponding dynamics is systematically investigated. The circuit consists of opamps, resistors, capacitors and a pair of semiconductor diodes connected in anti-parallel to synthesize the nonlinear component necessary for chaotic oscillations. The model is described by a continuous time three-dimensional autonomous system with hyperbolic sine nonlinearity, and may be viewed as a linear transformation of model MO15 previously introduced in [Sprott, 2010]. The structure of the equilibrium points and the discrete symmetries of the model equations are discussed. The bifurcation analysis indicates that chaos arises via the usual paths of period-doubling and symmetry restoring crisis. One of the key contributions of this work is the finding of a region in the parameter space in which the proposed (“elegant”) jerk circuit exhibits the unusual and striking feature of multiple attractors (i.e. coexistence of four disconnected periodic and chaotic attractors). Laboratory experimental results are in good agreement with the theoretical predictions.

Keywords: Jerk system with hyperbolic sine nonlinearity; electronic circuit implementation; routes to chaos; coexistence of multiple attractors; experimental study.

1. Introduction

It is well known that nonlinear dynamical systems can experience various forms of complexity including the possibility of bifurcation and chaos. The occurrence of two or more asymptotically stable equilibrium points or attracting sets (e.g. period- n limit cycle, torus, chaotic attractor) as the system parameters are being varied represents another striking and complex behavior observed in nonlinear systems. In a system developing coexisting attractors, the trajectories selectively converge on either of the attracting sets depending on the initial state of the system. Correspondingly, the basin of attraction of an attractive set is defined as the

set of initial points whose trajectories converge on the given attractor. The boundary separating each basin of attraction (i.e. separatrix) can be a smooth boundary or riddled basin with no clear demarcation (i.e. fractal). This striking and interesting phenomenon has been reported in various nonlinear systems including laser [Masoller, 1994], biological system [Cushing *et al.*, 2007; Upadhyay, 2003], chemical reactions [Massoudi *et al.*, 2010], Lorenz system [Li & Sprott, 2014], Newton–Leipnik system [Leipnik & Newton, 1981], and electrical circuits [Vaithianathan & Veijun, 1999; Kengne, 2015; Pivka *et al.*, 1994; Kuznetsov *et al.*, 2015; Kengne *et al.*, 2014], and so on. Such a phenomenon is mostly

connected to the system symmetry and may be accompanied by some special effects including for instance, symmetry-breaking bifurcation, symmetry restoring crisis, coexisting bifurcations, and hysteresis [Upadhyay, 2003; Pivka *et al.*, 1994; Kuznetsov *et al.*, 2015]. In practice, the coexistence of multiple attractors implies that an attractor may suddenly jump to a different attractor; the situation in which coexisting attractors possess fractal or intermingled basin of attraction being the most intriguing. In this case, due to noise, the observed signal may be the result of random switching of the system trajectory between two or more coexisting attractors.

In this work, we consider the dynamics of a simple autonomous jerk circuit which can be viewed as an analog computer of Model MO15 previously introduced in [Sprott, 2010]. Owing to the presence of the hyperbolic sine nonlinearity, this particular model is highly symmetric and thus shows potential to develop multiple coexisting attractors. First of all, let us recall that jerk systems [Sprott, 1997a, 1997b, 2000, 2010, 2011] are third-order differential equations of the form $\ddot{x} = J(\dot{x}, \dot{x}, x)$ where the nonlinear function $J(\cdot)$ is called the “jerk,” because it describes the third-time derivative of x , which would correspond to the first-time derivative of acceleration in a mechanical system. Previous works related to the coexistence of multiple attractors in simple jerk systems were carried out by Einchhorn and colleagues [Einchhorn *et al.*, 2002]. The authors investigated the dynamics that can be developed by two simplest polynomial jerk systems (that is JD1: $\ddot{x} = k_1\dot{x} + k_2x + \dot{x}\dot{x} + k_3$, and JD2: $\ddot{x} = k_1\dot{x} + k_2x + x^2 + k_3$) known to display chaotic dynamics in some ranges of their parameters. After deriving several analytical properties of these systems, the authors examined the dependence of the asymptotic dynamical behavior on the system parameters by numerical computation of the Lyapunov spectra. Furthermore, some features of the dependence on initial states (e.g. coexistence of two stable attractors, hysteresis) were also investigated based on forward and backward bifurcation diagrams. Due to the absence of any symmetry, not more than two coexisting solutions were found in both (JD1 and JD2) cases. Very recently, Kengne and colleagues [Kengne *et al.*, 2016] have performed a systematic analysis of a simple autonomous jerk system with cubic nonlinearity obtained by performing a linear transformation of Model MO5 first

introduced in [Sprott, 2010] prior to a more detailed analysis by Louodop and coworkers [Louodop *et al.*, 2014]. The basic dynamical properties of the system were investigated including equilibria and stability, phase portraits, frequency spectra, bifurcation diagrams and Lyapunov exponent plots. The main result of Kengne and collaborators was the finding of a window in the parameter space in which the jerk system (with cubic nonlinearity) experiences the unusual feature of multiple attractors (e.g. coexistence of four disconnected periodic and chaotic attractors). Among the very few cases of lower dimensional systems (e.g. Newton–Leipnik system [Leipnik & Newton, 1981]) capable of displaying such type of behavior, the jerk system with cubic nonlinearity was presented as the simplest and the most “elegant” prototype. An appropriate electronic circuit (the analog simulator) was designed and used for the investigations. Results of theoretical analyses were perfectly duplicated by laboratory experimental measurements. However, the main problem with Model MO5 is the presence of a cubic nonlinearity which is practically implemented by using two analog multipliers chips. Model MO15 in which the hyperbolic nonlinearity could be simply implemented with a pair of semiconductor diodes (connected in anti-parallel) represents a straightforward way to overcome this drawback, and thus may lead to a simpler electronic circuit realization [Sprott, 2011]. Motivated by the above results, the present work focuses on the dynamics of an electronic analog of Model MO15 with three keys objectives: (a) to perform a systematic analysis of the proposed jerk circuit and explain the chaos mechanism; (b) to define the region in the parameter space in which the proposed model exhibits multiple coexisting attractors and hysteresis; (c) to carry out an experimental study of the system to verify the theoretical analyses. The overall motivation of this work is to enrich in part the literature with a novel (simplest) chaotic system/circuit with multiple coexisting attractors; furthermore, we provide useful tools for the design of such types of oscillators for relevant engineering applications.

The paper’s structure is as follows. Section 2 deals with the modeling process. The electronic structure of the jerk circuit is presented and a suitable mathematical model is derived to describe the dynamics of the proposed oscillator. Some basic properties of the model are underlined. The stability of the equilibrium points is analyzed and conditions

for the occurrence of Hopf bifurcations are obtained. In Sec. 3, the bifurcation structures of the system are investigated numerically showing period-doubling and symmetry restoring crisis phenomena. A window (in the parameter space) corresponding to the occurrence of multiple coexisting attractors is revealed. Correspondingly, basins of attraction of various coexisting solutions are computed showing complex basin boundaries. The experimental study of the oscillator is carried out in Sec. 4. Laboratory experimental measurements show a very good agreement with the theoretical analyses. Finally some concluding remarks and proposal for future work are drawn in Sec. 5.

2. Description and Analysis of the Model

2.1. Circuit description

The schematic diagram of the proposed jerk circuit is depicted in Fig. 1. The circuit consists of three successive integrators in a multiple feedback loop in addition to a nonlinear feedback loop involving a negative gain amplifier with a pair of semiconductor diodes (D_1, D_2). The circuit can be scaled over a wide range of frequencies provided an appropriate choice of capacitors' values. A symmetrical characteristic [Buscarino *et al.*, 2012] is obtained by connecting two diodes in anti-parallel, i.e. with the two terminals shortened but with opposite polarities. In such type of configuration, the voltage across each

diode is equal to the voltage of the resulting two-terminal device, while the current is the sum of the current flowing through each diode. This symmetrical nonlinearity is necessary for the occurrence of symmetric (by inversion with respect to the origin) attractors [Buscarino *et al.*, 2012]. Assuming ideal op. amplifiers (operating in their linear regions), we would like to mention that the pair of semiconductor diodes are the only nonlinear elements responsible for the chaotic behavior displayed by the complete electronic generator.

2.2. State equations

In order to derive a mathematical model of the proposed Jerk system, some useful assumptions are considered. First, we assume linear capacitors and ideal opamps operating in their linear working domain. Second, the current-voltage characteristic ($I-V$) of the pair of semiconductor diodes (D_1 and D_2) is obtained from the Shockley diode equation [Hania *et al.*, 2006; Sukov *et al.*, 1997] as follows:

$$\begin{aligned} I_d &= I_{D_1} - I_{D_2} \\ &= I_S \left[\exp\left(\frac{V_d}{\eta V_T}\right) - 1 \right] - I_S \left[\exp\left(\frac{-V_d}{\eta V_T}\right) - 1 \right] \\ &= 2I_S \sinh\left(\frac{V_d}{\eta V_T}\right) \end{aligned} \quad (1)$$

where I_S is the saturation current of the junction; $V_T = k_b T/q$ is the thermal voltage with k_b the

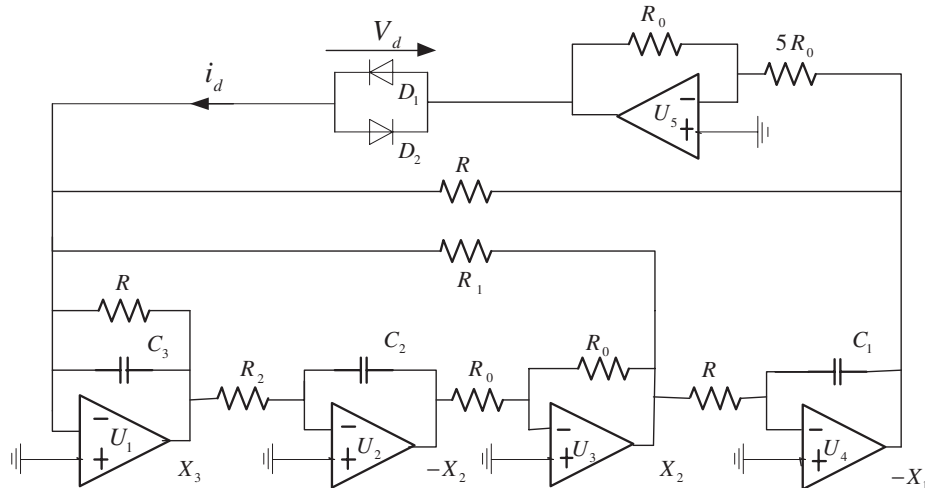


Fig. 1. Electronic circuit realization of the jerk system with hyperbolic sine nonlinearity. The simplicity of the model is remarkable. The pair of semiconductor diodes implement the hyperbolic nonlinearity of the model. The following values of electronic circuit components are used for the analysis: $R = 50 \text{ k}\Omega$, $C_1 = C_2 = C_3 = C = 2 \text{ nF}$, $R_0 = 10 \text{ k}\Omega$, R_1 – tuneable, R_2 – tuneable, a pair of general purpose signal diodes $D_1 = D_2 = 1N4148$ ($\eta = 1.9$, $V_T = 26 \text{ mV}$, $I_S = 2.682 \text{ nA}$), $U_j(j = 1, 2, 3, 4) = TL084CN$, $U_5 = TL082CN$.

Boltzmann constant, T the absolute temperature expressed in Kelvin, q the electron charge and η is the ideality factor ($1 < \eta < 2$). With the above assumptions, it can be shown that the voltages X_1, X_2 and X_3 satisfy the following set of three coupled first-order nonlinear differential equations:

$$\left\{ \begin{array}{l} \frac{dX_1}{dt} = \frac{X_2}{RC} \\ \frac{dX_2}{dt} = \frac{X_3}{R_2C} \\ \frac{dX_3}{dt} = \frac{X_1}{RC} - \frac{X_2}{R_1C} - \frac{X_3}{RC} \\ \quad - \frac{2I_S \sinh\left(\frac{X_1}{5\eta V_T}\right)}{C} \end{array} \right. \quad (2)$$

With the adoption of the following change of variables and parameters: $X_k = x_k \times 1V (k = 1, 2, 3)$,

$$\begin{aligned} t &= \tau RC, \quad \sigma = \frac{R}{R_2}, \quad \gamma = \frac{R}{R_1}, \\ \rho &= \frac{1V}{5\eta V_T}, \quad \varepsilon = \frac{2RI_S}{1V} \end{aligned} \quad (3)$$

the normalized circuit equations are expressed by the following smooth nonlinear third-order differential equations convenient for numerical integration:

$$\left\{ \begin{array}{l} \dot{x}_1 = x_2 \\ \dot{x}_2 = \sigma x_3 \\ \dot{x}_3 = x_1 - \gamma x_2 - x_3 - \varepsilon \sinh(\rho x_1) \end{array} \right. \quad (4)$$

where the dot denotes differentiation with respect to the dimensionless time. It can be seen that only one state variable (namely x_1) is involved in the hyperbolic nonlinearity of the model. Note that the presence of this nonlinearity is responsible for the complex behaviors exhibited by the whole system. In the mathematical model in (4), four parameters can be identified. Two of them (namely ε and ρ) depend on intrinsic diode parameters and thus will be kept constant during all the numerical analyses: $\varepsilon = 2.682 \times 10^{-4}$, $\rho = 4.0485$. Therefore, the bifurcation analysis of the system will be carried out in terms of the control parameters σ and γ respectively (i.e. with respect to R_1 and R_2). The values of electronic components used for the numerical analysis are listed in the caption of Fig. 1. We would like to let the reader notice that there are in fact only

three independent parameters as can be seen by making the transformation $x_k \rightarrow x_k/\rho (k = 1, 2, 3)$, which reduces it to a system in which only the product $\varepsilon\rho$ appears. However, we have kept the model in (4) since both ε and ρ are held fixed throughout the rest of the paper. Mention that system (4) can be expressed equivalently in the general jerk form as follows:

$$\ddot{x} = -\sigma\gamma\dot{x} - \ddot{x} + \sigma x - \sigma\varepsilon \sinh(\rho x). \quad (5)$$

Equation (5) shows that our model belongs to the wider class of “elegant” jerk dynamical systems defined in [Sprott, 2010]. Furthermore, our model (4) represents one of the simplest autonomous 3D system reported to date, capable of displaying four disconnected chaotic and periodic attractors (see Secs. 3 and 4) depending solely on the initial states [Sprott, 2010; Malasoma, 2000; Eichhorn et al., 2002]. It should also be stressed that the form of Eq. (5) is such that the coefficient of the hyperbolic term is an amplitude parameter, which allows simple control of the signal amplitude in the electrical circuit through a single resistor as described in [Li & Sprott, 2013b; Li et al., 2015a]. Also mention that the circuit in Fig. 1 can be significantly simplified by replacing U2 and U3 and their associated resistors and capacitors with a single RC element as shown in Fig. 10.21 of [Sprott, 2010]. However, we prefer the circuit of Fig. 1 as it is easily adjustable to display the complex phenomena discussed in this work.

2.3. Symmetry

System (4) is invariant under the transformation: $(x_1, x_2, x_3) \Leftrightarrow (-x_1, -x_2, -x_3)$. Thus, if (x_1, x_2, x_3) is a solution of system (4) for a given set of parameters, then $(-x_1, -x_2, -x_3)$ is also a solution for the same parameter set. A solution of (4) that is invariant under the transformation is called a symmetric solution; otherwise it is called an asymmetric solution. The equilibrium point $P_0(0, 0, 0)$ is a trivial symmetric static solution. Consequently, attractors in state space have to be symmetric by inversion with respect to the origin; otherwise they must appear in pairs, to restore the exact symmetry of the model equations. This exact symmetry could serve to justify the occurrence of multiple co-existing attractors in state space. Furthermore, it may be helpful to check the scheme used for numerical computations.

2.4. Dissipation and existence of attractors

Preliminary information concerning the existence of attractive sets of our model could be obtained by evaluating the volume contraction rate ($\Lambda = V^{-1}dV/dt$) of the oscillator described by (4) at any given point $x = (x_1, x_2, x_3)^T$ of the state space [Strogatz, 1994; Argyris *et al.*, 1994; Nayfeh & Balachandra, 1995]. The following expression can be easily derived:

$$\Lambda = \frac{\partial \dot{x}_1}{\partial x_1} + \frac{\partial \dot{x}_2}{\partial x_2} + \frac{\partial \dot{x}_3}{\partial x_3} = -1. \quad (6)$$

It follows that Λ is negative independently of the position x in state space. Hence system (4) is dissipative. This implies that any volume element $V_0 = V(t=0)$ will be continuously contracted by the flow. In other words, each volume element containing the trajectory shrinks to zero as time evolves (i.e. $t \rightarrow \infty$). As a result, all system orbits will be confined to a specific bounded subset of zero volume in state space and the asymptotic dynamics converges to an attractor.

2.5. Fixed point analysis

It is well known that the equilibrium points play a crucial role on the dynamics of a nonlinear system [Strogatz, 1994; Argyris *et al.*, 1994; Nayfeh & Balachandra, 1995]. By setting the right-hand side of system (4) to zero, it can be easily shown that there are three fixed points: $P_0 = (0, 0, 0)$ and $P_{1,2} = (\pm\alpha, 0, 0)$ where α is the solution of the transcendental equation:

$$\alpha - \varepsilon \sinh(\rho\alpha) = 0. \quad (7)$$

With the set of system parameters defined above, we have solved numerically Eq. (7) using the MATLAB built-in function “fzero”; the approximate value of the obtained solution is $\alpha \approx 2.4209$. Note that P_1 and P_2 are symmetric with respect to the origin; consequently they share the same stability properties. It should also be stressed that the location in state space of the three fixed points is independent of the pair of control parameters (σ, γ) . The Jacobian matrix of system (4) evaluated at any equilibrium point $(\bar{x}_1, \bar{x}_2, \bar{x}_3)$, is expressed as follows:

$$M_J = \begin{bmatrix} 0 & 1 & 0 \\ 0 & 0 & \sigma \\ 1 - \varepsilon\rho \cosh(\rho\bar{x}_1) & -\gamma & -1 \end{bmatrix}. \quad (8)$$

The eigenvalues related to the above matrix can be found by solving the following characteristic equation ($\det(M_J - \lambda I_d) = 0$):

$$\lambda^3 + \lambda^2 + \sigma\gamma\lambda - \sigma(1 - \varepsilon\rho \cosh(\rho\bar{x}_1)) = 0 \quad (9)$$

where I_d is the 3×3 identity matrix. Provided that $\varepsilon\rho \ll 1$, according to the Lyapunov stability theory, $P_0(0, 0, 0)$ is always unstable since the corresponding characteristic equation has coefficients with different signs. In contrast, the stability of both nontrivial equilibrium points $(P_{1,2})$ strongly depends on the two control parameters σ and γ . Following the Routh–Hurwitz stability criterion [Strogatz, 1994], we have found that both P_1 and P_2 are stable only for $\gamma > \gamma_c = \varepsilon\rho \cosh(\rho\alpha) - 1$. However, this state of nonoscillation can be broken if the control parameter γ is decreased beyond the critical value γ_c . Correspondingly, the Hopf bifurcation conditions have been computed as follows:

$$\gamma_c = \varepsilon\rho \cosh(\rho\alpha) - 1, \quad \omega_{\text{Hopf}} = \sqrt{\gamma\sigma} \quad (10a)$$

$$\text{Re} \left(\frac{d\lambda}{d\gamma} \Big|_{\gamma=\gamma_c} \right) = \frac{-\sigma}{2(1 - \sigma + \sigma\varepsilon\rho \sinh(\rho\alpha))} \neq 0. \quad (10b)$$

Equation (10a) provides the frequency of stable oscillations as well as the critical value of γ corresponding to the Hopf bifurcation of the system. From Eq. (10b), it can be seen that the transversality condition is always fulfilled provided that σ is a positive control parameter. From the above discussion, it follows that in the regime of (regular or chaotic) oscillations, the three equilibria are unstable, and thus the system generates self-excited oscillations [Leonov & Kuznetsov, 2013; Leonov *et al.*, 2015]. For instance, considering the particular case of $(\sigma, \gamma) = (9.3, 2.0)$ for which the system develops four distinct (chaotic and periodic) attractors (see Sec. 4) the eigenvalues evaluated at P_0 are $\lambda_1 = 0.4810$, $\lambda_{2,3} = -0.7405 \pm j4.3318$ whereas those at $P_{1,2}$ are $\lambda_1 = -3.1953$, $\lambda_{2,3} = 1.0976 \pm j4.9406$. This clearly shows that the three fixed points are all unstable (presence of eigenvalues with positive real part) in the regime of multiple attractors, which is synonymous of self-excited oscillations.

3. Numerical Study

3.1. Computational methods

In order to explore the rich variety of bifurcation modes that can be observed in the novel

autonomous jerk system, we solve numerically system (4) using the standard fourth-order Runge–Kutta integration algorithm. For each set of parameters used in this paper, the time step is always $\Delta t = 2 \times 10^{-3}$ and the computations are carried out using variables and constant parameters in extended mode (Turbo Pascal codes). For each parameters setting, the system is integrated for a sufficiently long time and the transient is ignored. Two indicators are substantially exploited to characterize the type of transition leading to chaos. The bifurcation diagram represents the first indicator, the second indicator being the graph of largest 1D Lyapunov exponent (λ_{\max}). Concerning the latter indicator, the dynamics of the system is classified based on its Lyapunov exponent which is computed numerically using the algorithm described by Wolf and co-workers [Wolf *et al.*, 1985]. In particular, the sign of the largest Lyapunov exponent determines the growth rate of almost all small perturbations to the system's state, and consequently, the nature of the underlined dynamical attractor. For $\lambda_{\max} < 0$ all perturbations vanish and trajectories starting sufficiently close to each other converge to the same stable equilibrium point in state space; for $\lambda_{\max} = 0$, initially close orbits remain close but distinct, corresponding to oscillatory motion on a limit-cycle or torus; and finally for $\lambda_{\max} > 0$, small perturbations grow exponentially, and the system evolves chaotically within the folded space of a strange attractor. To gain further insight about the complex dynamics of the jerk system, we plot the Poincaré sections of attractors as well as related frequency spectra. Concerning the latter case, it should be recalled that for periodic motion, all spikes in the power spectrum are harmonically related to the fundamental whereas a broadband power spectrum is characteristic of a chaotic mode of oscillations. Briefly recall that the periodicity of the attractor is deduced by counting the number of spikes located on the left hand-side of the highest spike of the spectrum (the latter being included).

3.2. Route to chaos

In order to investigate the sensitivity of the jerk system in terms of a single bifurcation parameter, we fix $\gamma = 2.0$ and vary σ in the range $1.0 \leq \sigma \leq 20.0$. We found that the jerk system under scrutiny can exhibit very rich and striking bifurcation sequences when slowly adjusting the bifurcation parameter. Sample results showing

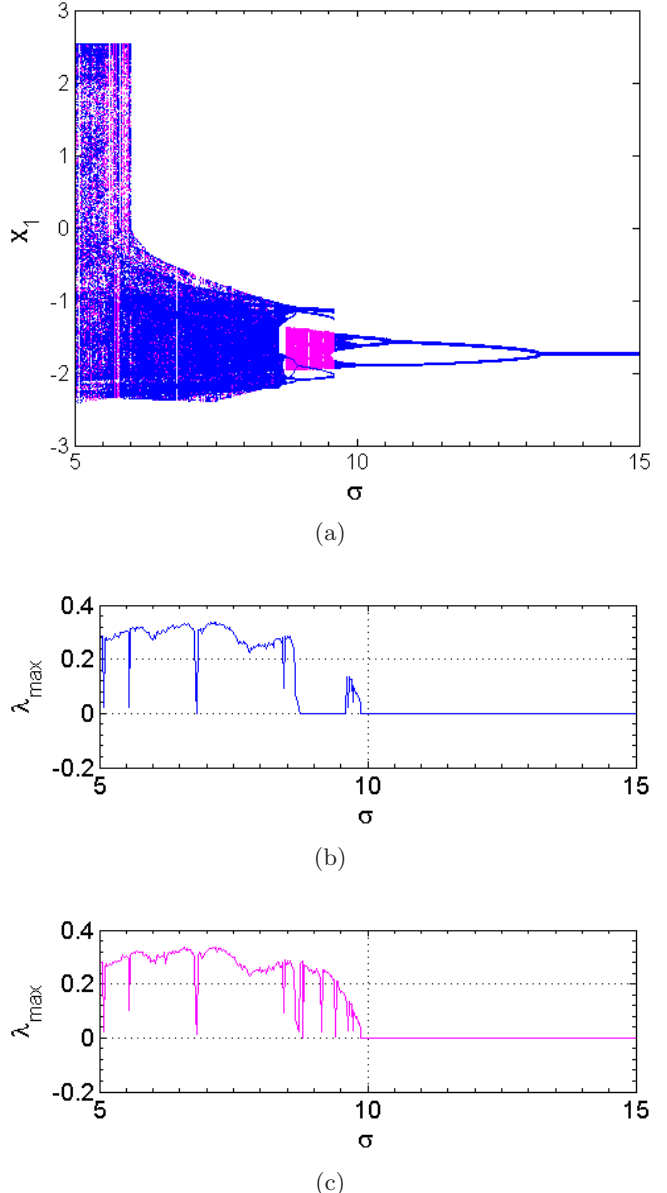


Fig. 2. (a) Bifurcation diagram showing local maxima of the coordinate x_1 versus σ and (b), (c) the corresponding graphs of largest 1D Lyapunov exponent (λ_{\max}) plotted in the range $5 \leq \sigma \leq 15$. A window of hysteretic dynamics can be noticed.

the bifurcation diagram for varying σ and the corresponding graphs of largest 1D Lyapunov exponent are provided in Figs. 2(a)–2(c) respectively. The bifurcation diagram is obtained by plotting local maxima of the coordinate $x_1(\tau)$ versus the bifurcation control parameter that is increased (or decreased) in small steps in the range $5.0 \leq \sigma \leq 15.0$. The final state at each iteration of the bifurcation control parameter is used as the initial condition for the next iteration. Two sets of data corresponding respectively for increasing (blue) and

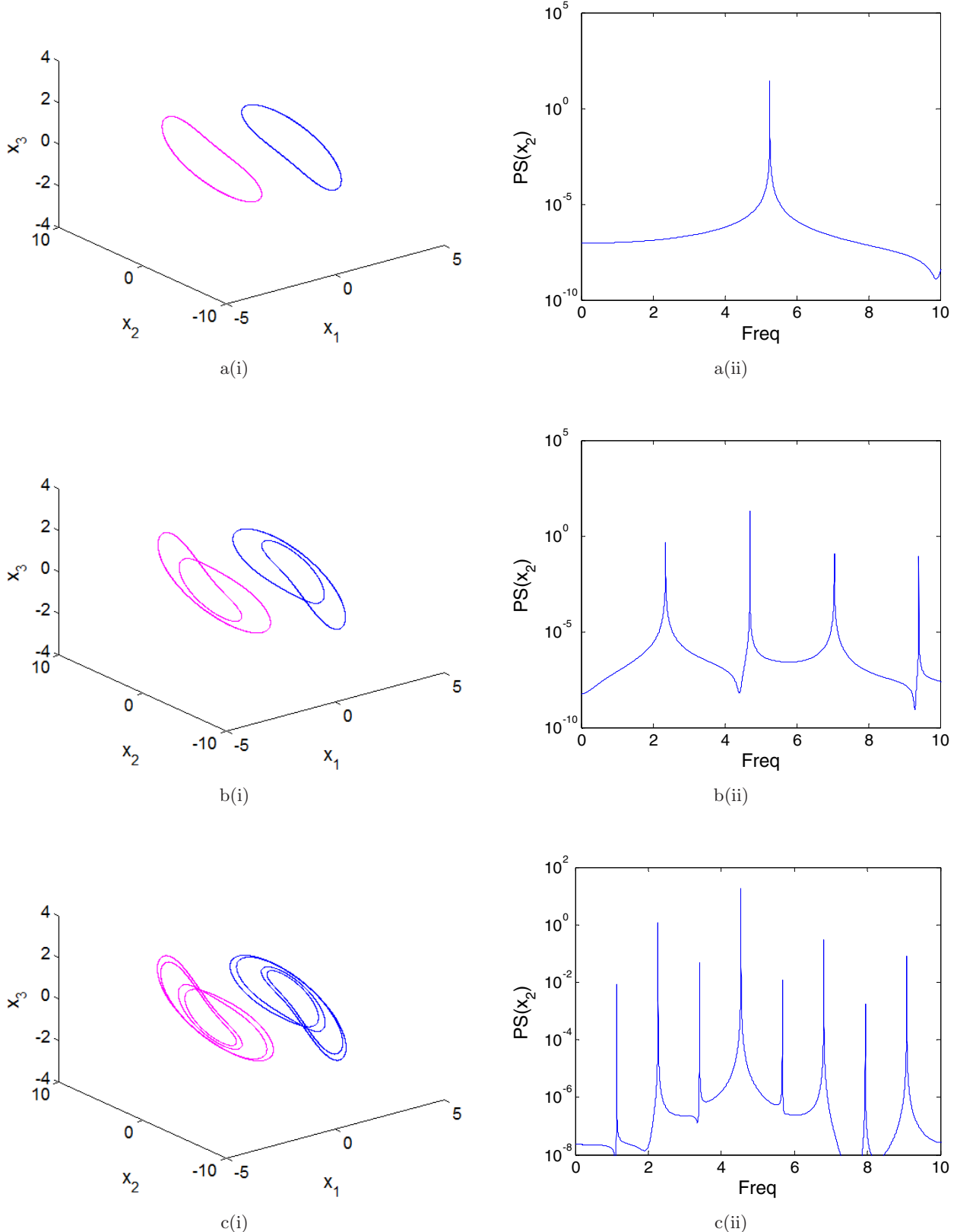
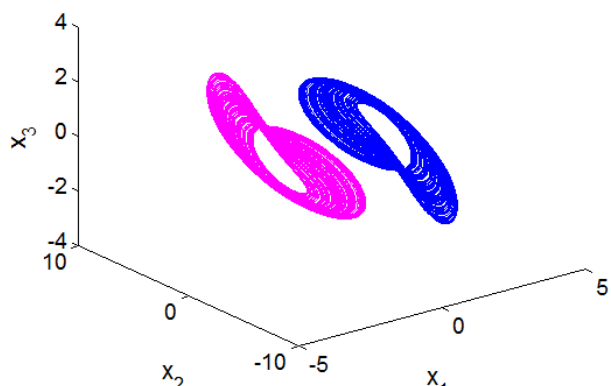
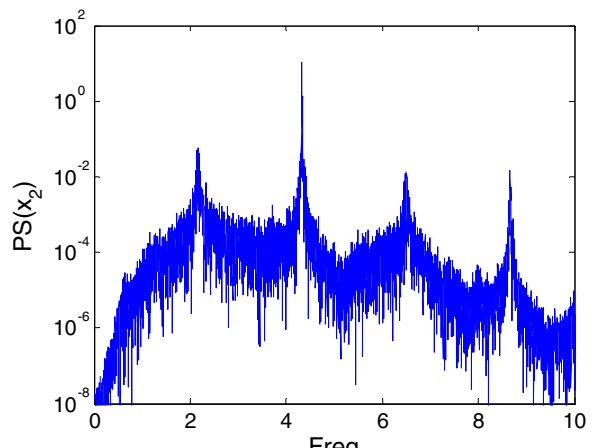


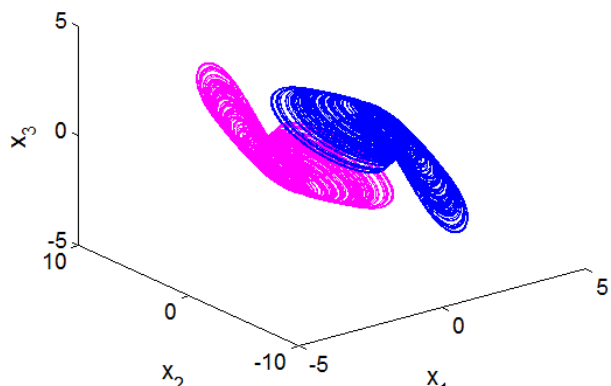
Fig. 3. Phase space trajectories (left) and corresponding frequency spectra (right) showing routes to chaos in the system for varying σ : (a) Period-1 for $\sigma = 14$, (b) period-2 for $\sigma = 11$, (c) period-4 for $\sigma = 10.2$, (d) single-band spiraling chaos for $\sigma = 9.3$, (e) single-band screw-like chaos for $\sigma = 8$, (f) double-band chaotic attractor for $\sigma = 5.4$. Pairs of asymmetric attractors are obtained using (noncritical) initial conditions $(x_1(0), x_2(0), x_3(0)) = (\pm 2, 0, 0)$.



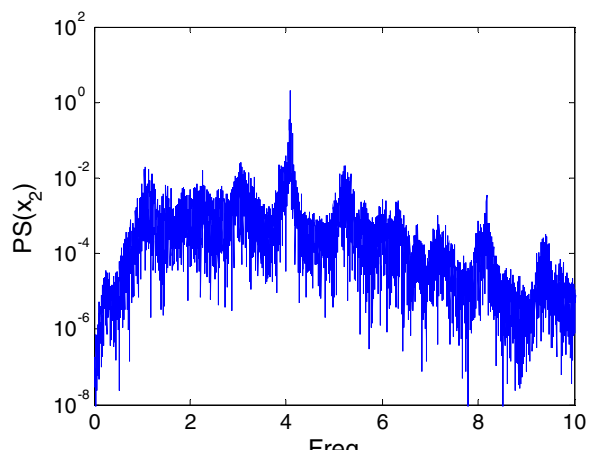
d(i)



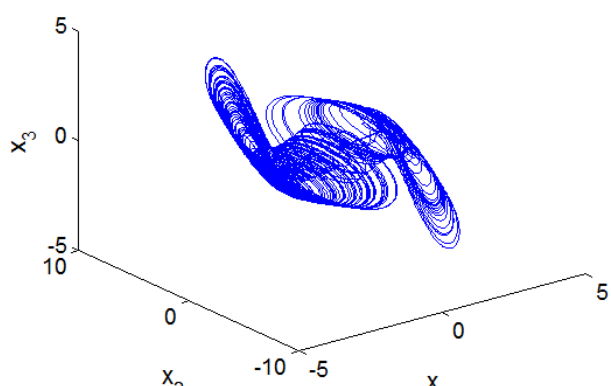
d(ii)



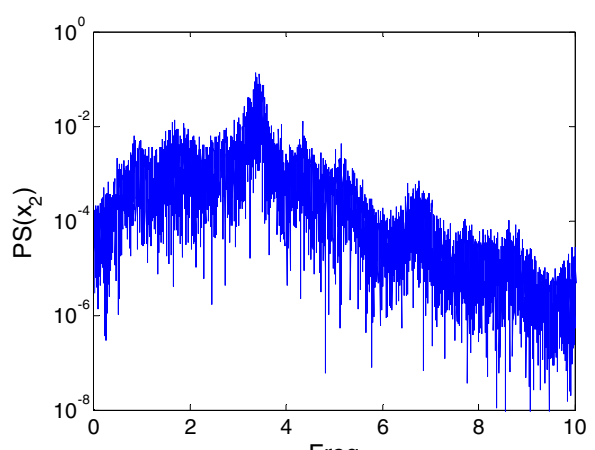
e(i)



e(ii)



f(i)



f(ii)

Fig. 3. (Continued)

decreasing (magenta) values of σ are superimposed in the graph of Fig. 2(a). This strategy represents a straightforward method to identify the domain in which the jerk system demonstrates multiple coexisting attractors' behavior (see Sec. 4). From Figs. 2(a) and 2(b), the following bifurcation sequence can be captured when the bifurcation control parameter σ is slowly decreased. First, for values of σ above the critical values $\sigma_{\text{cr}1} = 13.22$, the system exhibits a limit cycle motion. When decreasing the control parameter σ past this critical value, the stable period-1 limit cycle undergoes a series of period-doubling bifurcation culminating to a single-band spiraling (Feigenbaum) chaotic attractor. Further decreasing σ down to $\sigma_{\text{cr}2} \approx 8.74$, the spiraling chaotic attractor suddenly collapses, giving rise to another spiraling-like chaotic one of

larger size and different shape. Past the critical value $\gamma_{\text{cr}3} = 8.60$, the latter spiraling chaotic attractor suddenly changes to a screw (Shilnikov)-like chaotic attractor. A double-band chaotic attractor is observed at $\sigma_{\text{cr}4} \approx 6.0$ as a result of a symmetry recovering crisis. It can be seen that the bifurcation diagram well coincides with the graph of the largest Lyapunov exponent (λ_{\max}). With the same set of parameters in Fig. 2, various numerical phase portraits as well as corresponding frequency spectra were computed to support different bifurcation scenarios depicted previously (see Fig. 3). Asymmetric attractor pairs are observed in Figs. 3(ai)–3(ei) while a double-band strange attractor is depicted in Fig. 3(f). To gain more insight about the complexity of the attractor depicted in Fig. 3(f), various two-dimensional projections are presented in Fig. 4.

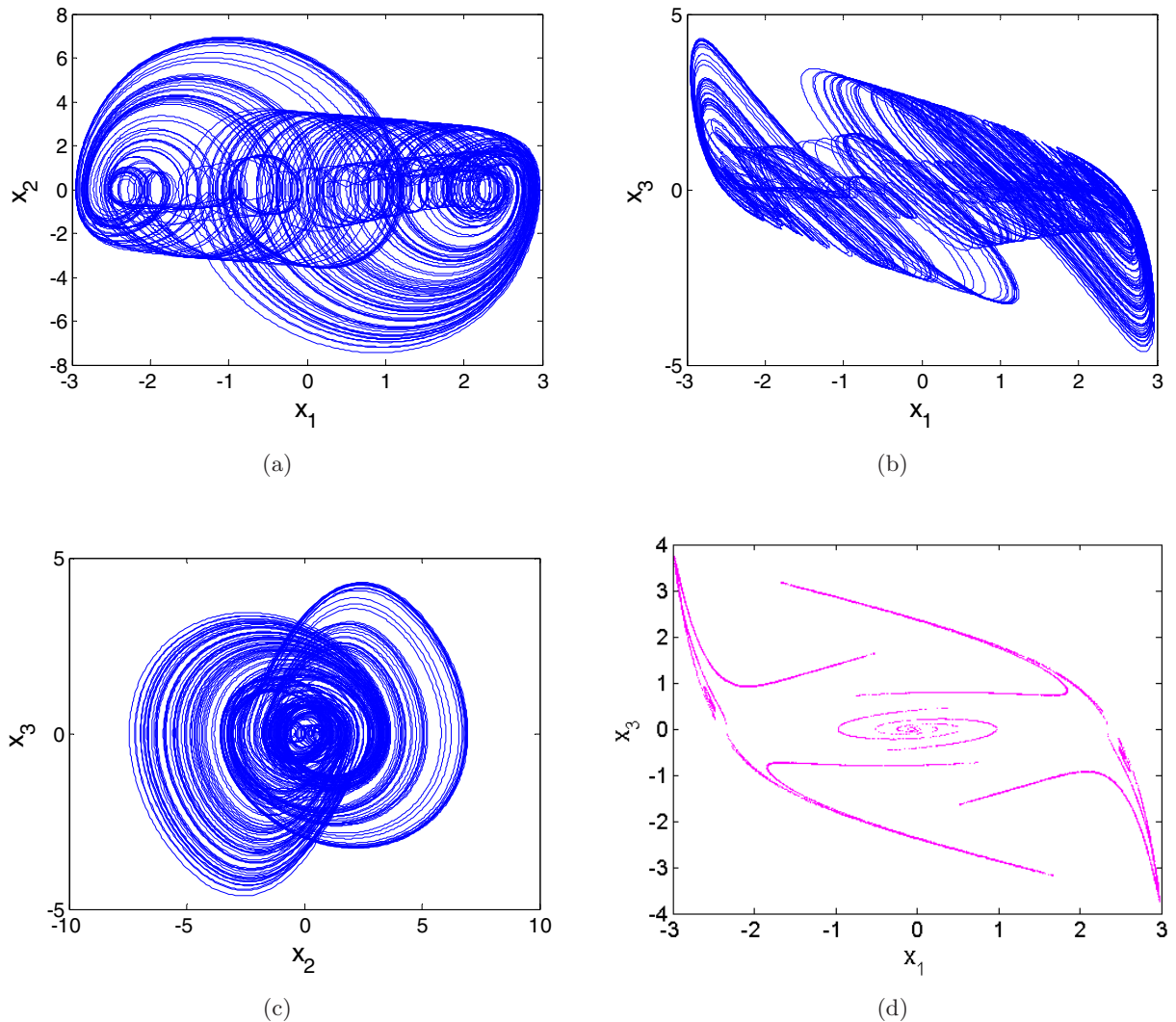


Fig. 4. (a)–(c) Two-dimensional projections of the double-band chaotic attractor illustrating the complexity of the system and (d) corresponding double-sided Poincaré section in the plane $x_1 = 0$. Parameters are those in Fig. 3(f).

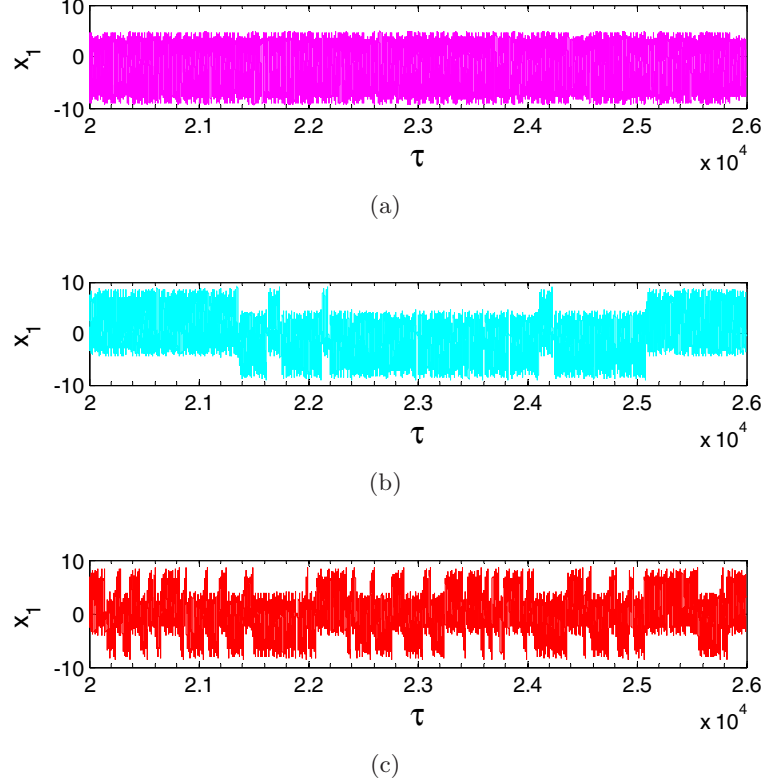


Fig. 5. Illustration of the symmetry restoring crisis for $\sigma < \sigma_c \approx 6.0$, there are two mirror image chaotic attractors, one with $x_1(\tau) < 0$ and one with $x_1(\tau) > 0$. The two attractors merge to form unique attractor with mirror symmetry at $\sigma = \sigma_c \approx 6$. The figure depicts: (a) the time series of the attractor with negative mean value for $\sigma = 8.0$; (b) and (c) the time series of the attractor for $\sigma = 5.9$ and $\sigma = 5.5$ (respectively) past the symmetry restoring crisis.

In the same line, the Poincaré section of the attractor is shown in Fig. 4(d). The shape of this Poincaré section is characteristic of chaotic attractors. Furthermore, we provide in Fig. 5 the time traces of

the coordinate $x_1(\tau)$ to illustrate the crisis induced intermittency experienced by the system.

The Hopf type bifurcation, the period-doubling scenario to chaos, and the symmetry restoring crisis

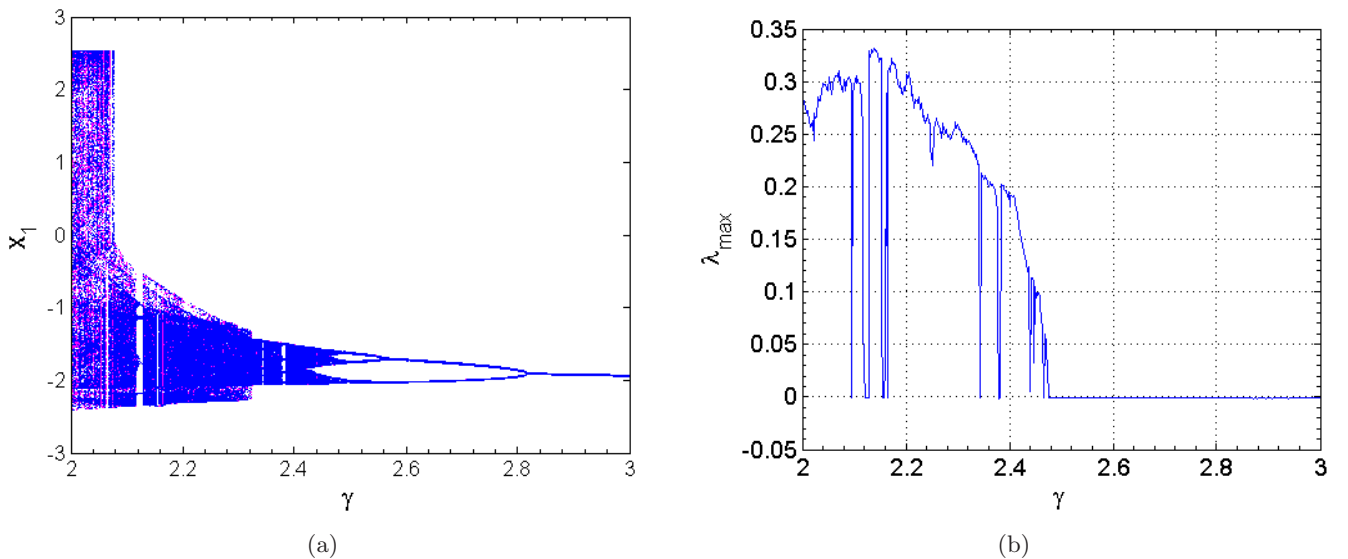


Fig. 6. (a) Bifurcation diagram showing local maxima of the coordinate x_1 versus γ and (b) the corresponding graph of largest Lyapunov exponent (λ_{\max}) plotted with $\sigma = 5.0$, in the range $2 \leq \gamma \leq 3$.

are observed when using γ as bifurcation control parameter (see Fig. 6). In particular, setting $\sigma = 5.0$, it is found that the system moves from the state of fixed point motion to the oscillation regime as the result of a Hopf bifurcation (see Sec. 2.2) when decreasing γ beyond the threshold value $\gamma_c \approx 8.800$. Also, it ought to be stressed that the routes to chaos observed in this work have also been reported in various nonlinear systems including, for instance, the second-order nonautonomous Duffing oscillator [Nayfeh & Balachandran, 1995] and Chua's circuit [Swathy & Thamilmaran, 2013]. A two-parameters diagram showing regions of irregular behavior (chaos) in the (γ, σ) plane is depicted in Fig. 7. This diagram is of great importance for a practical circuit design of a physical jerk circuit.

3.3. Occurrence of multiple attractors

With reference to the bifurcation diagram of Fig. 2 and corresponding zoom depicted in Fig. 8, a window of hysteretic dynamics (and thus multiple stability) can be identified in the range $8.74 \leq \sigma \leq 9.62$ (see Fig. 5). For values of σ within this range, the long term behavior of the system depends on initial states thus leading to the interesting and striking phenomenon of coexisting multiple attractors' behavior. Up to four different attractors (see Fig. 9) can be obtained depending solely on the choice of initial conditions. For example, the chaotic phase

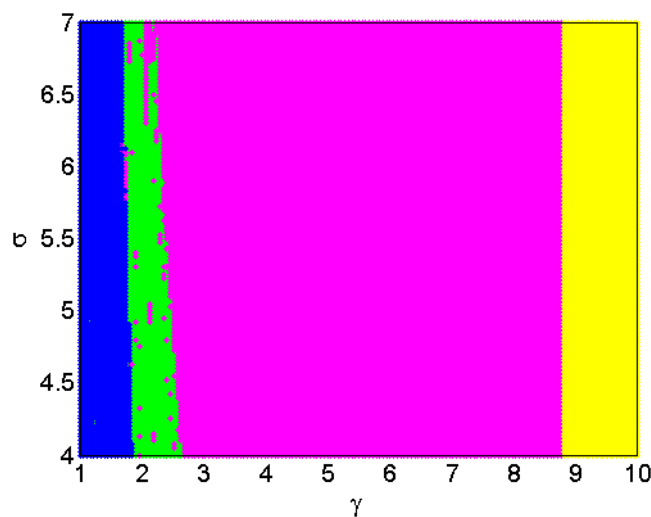


Fig. 7. Two-parameters phase diagram in the (γ, σ) plane showing respectively: the region of nonoscillations (yellow), the region of periodic dynamics (magenta), the region of chaotic dynamics (green), and the region of unbounded dynamics (blue).

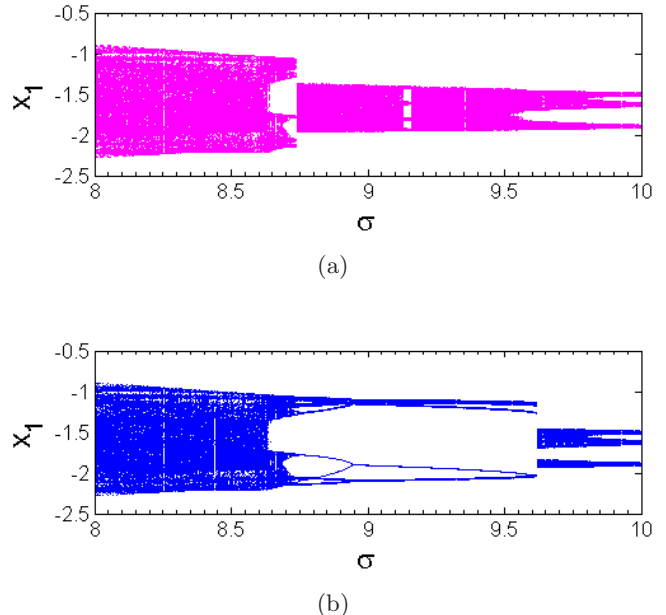


Fig. 8. Enlargement of the bifurcation diagram of Fig. 2 showing the region in which the system exhibits multiple coexisting attractors. This region corresponds to values of σ in the range: $8 \leq \sigma \leq 10$. Two sets of data corresponding respectively to increasing (magenta) and decreasing (blue) values of the bifurcation control parameter are superimposed.

portraits of Fig. 9(a) can be obtained under the initial conditions $x_1(0) = 0, x_2(0) = 0, x_3(0) = \pm 0.1$; using the initial point $x_1(0) = 0, x_2(0) = 0, x_3(0) = \pm 1$, a completely different attractor (i.e. period-3 limit cycles) is obtained in Fig. 9(b). Therefore, using the same parameters setting in Fig. 9 and carrying out a scan of initial conditions (see Fig. 10), we have defined the domain of initial conditions in which each attractor can be obtained. The complexity of the basin boundaries is clearly illustrated in Fig. 10 where cross-sections of the basins of attraction are depicted, respectively, for $x_1(0) = 0, x_2(0) = 0$, and $x_3(0) = 0$ associated to the symmetric pair of limit cycles (blue and yellow) and the pair of chaotic attractors (green and magenta). Red zones correspond to unbounded motion. It should be mentioned that, according to the best of the author's knowledge, the striking phenomenon of multiple stability involving four disconnected coexisting attractors, previously observed in the Leipnik–Newton system [Leipnik & Newton, 1981] and very recently in a linear transformation of jerk system Model MO5 [Kengne *et al.*, 2016], has not yet been reported in any other jerk system, and thus represents an enriching contribution related to the dynamic behavior of this large class of nonlinear

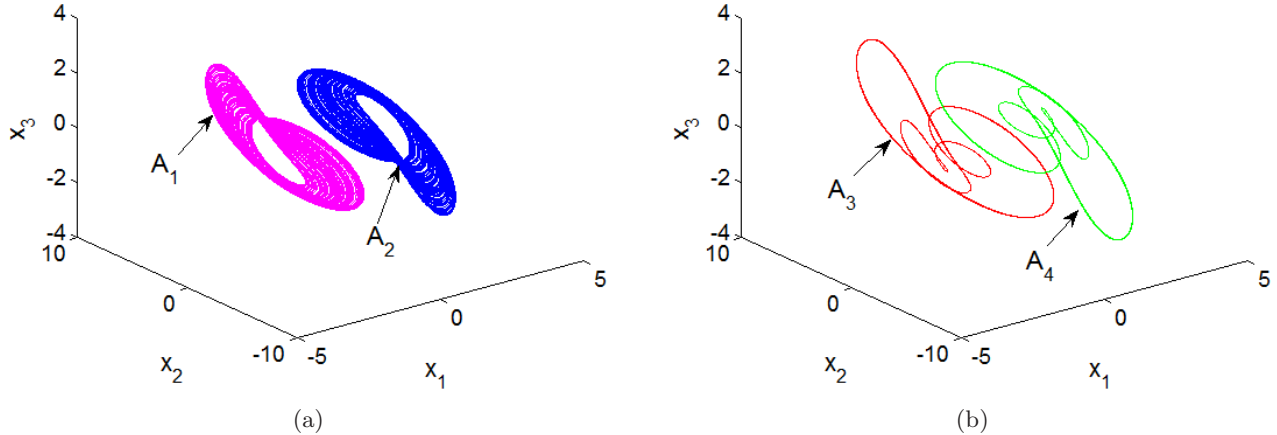


Fig. 9. Coexistence of four different attractors (a pair of period-4 limit cycles and a pair of chaotic attractors) for $\gamma = 2$, $\sigma = 9.3$. Initial conditions $(x_1(0), x_2(0), x_3(0))$ are $(0, 0, \pm 0.1)$ and $(0, 0, \pm 1)$ respectively.

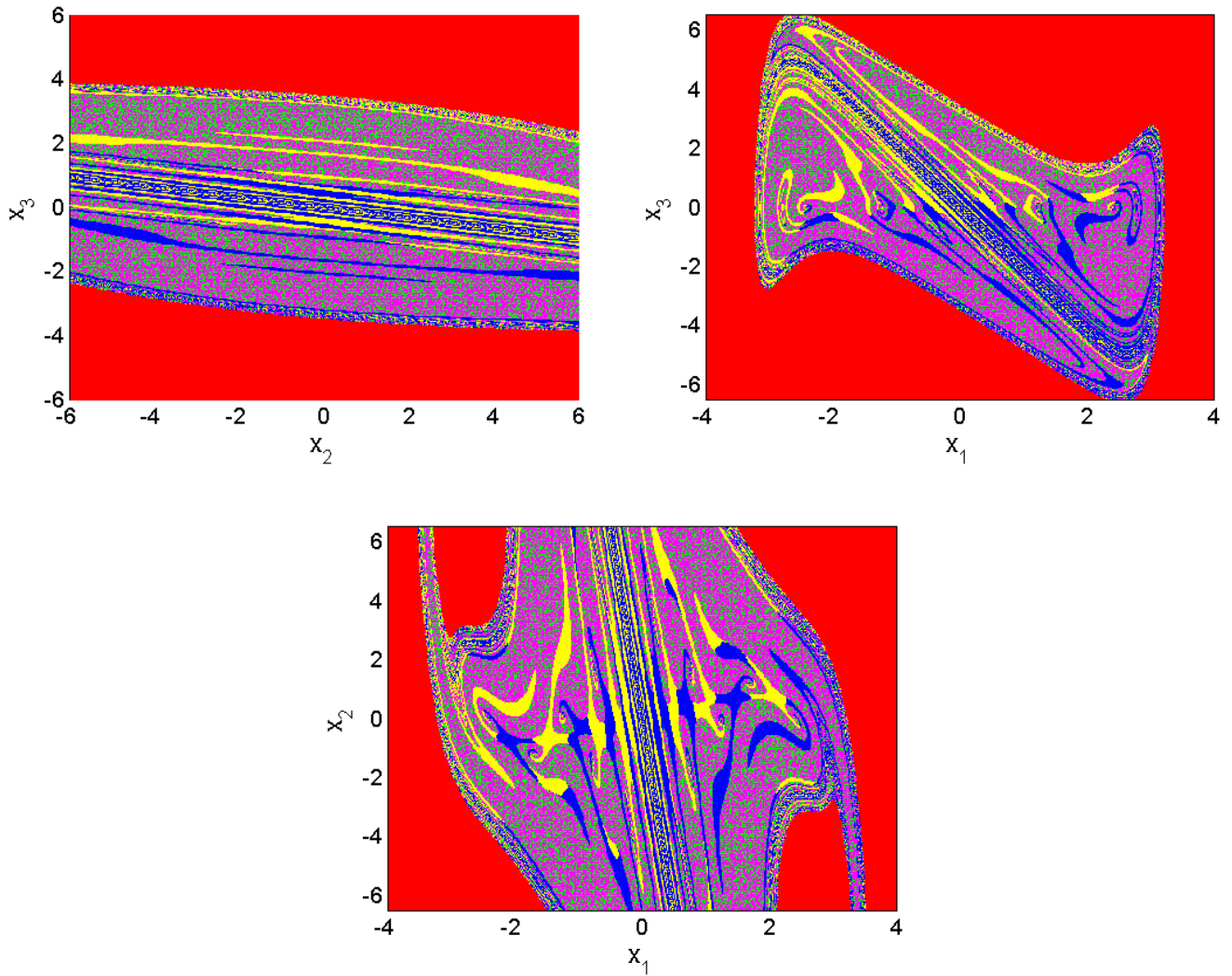


Fig. 10. Cross-sections of the basin of attraction for $x_1(0) = 0$, $x_2(0) = 0$ and $x_3(0) = 0$ respectively, corresponding to the asymmetric pair of period-4 cycle (blue and yellow) and the pair of chaotic attractors (green and magenta) obtained for $\gamma = 2$, $\sigma = 9.3$. Red regions correspond to unbounded motion.

systems. It should also be noted that multiple attractors behavior (involving less than four non-static attractors) are encountered in other nonlinear systems including laser [Masoller, 1994], biological system [Cushing *et al.*, 2007; Upadhyay, 2003], Lorenz system [Li & Sprott, 2014], and electrical circuits [Vaithianathan & Veijun, 1999; Kengne, 2015; Pivka *et al.*, 1994; Kuznetsov *et al.*, 2015; Kengne *et al.*, 2014; Maggio *et al.*, 1999], and so on. The case of coexistence of infinitely many attractors, also referred to as extreme multistability, arising in coupled dynamical systems was recently discussed by Hens and co-workers [Hens *et al.*, 2015]. Provided that the occurrence of multiple attractors represents an additional source of randomness [Luo & Small, 2007], some obvious potential applications include, for instance, chaos-based secure communication as well as random bit generation. However, this singular type of behavior is not desirable in general, and justifies the need for control. Detailed analysis on this line is beyond the scope of this contribution; also, interested readers are guided to the interesting review paper on control of multistability presented in [Pisarchik & Feudel, 2014].

4. Experimental Study

Following the above theoretical analysis, it is predicted that the jerk system under investigation can exhibit very rich and complex behaviors. Our goal in this section is to validate the theoretical results obtained previously by performing an experimental study of the real system [Kiers & Schmidt, 2004; Kingni *et al.*, 2013; Kingni *et al.*, 2014]. To this end, the schematic diagram of Fig. 1 is constructed on a breadboard (see Fig. 11). The circuit is built using TL084 and TL082 op. amplifiers type with a symmetric ± 15 V dc voltage supply. The same values of electronics components used for the numerical study are kept here to enable the comparison process. The experimental results are obtained (with $R_1 = 25\text{ k}\Omega$) by slowly increasing R_2 (i.e. decreasing parameter σ) and plotting phase-space trajectories (X_2, X_1) using a dual trace oscilloscope in the XY mode. When slowly monitoring the control resistor R_2 , we found that the experimental jerk circuit experiences various types of bifurcation. For $R_2 = 1\text{ k}\Omega$ a period-1 limit cycle is observed. When R_2 is gradually increased, the complete sequence of bifurcation reported above is observed: period-1 \rightarrow period-2 \rightarrow period-4 \rightarrow period-8 \rightarrow spiraling one-band attractor \rightarrow screw-like one-band chaotic

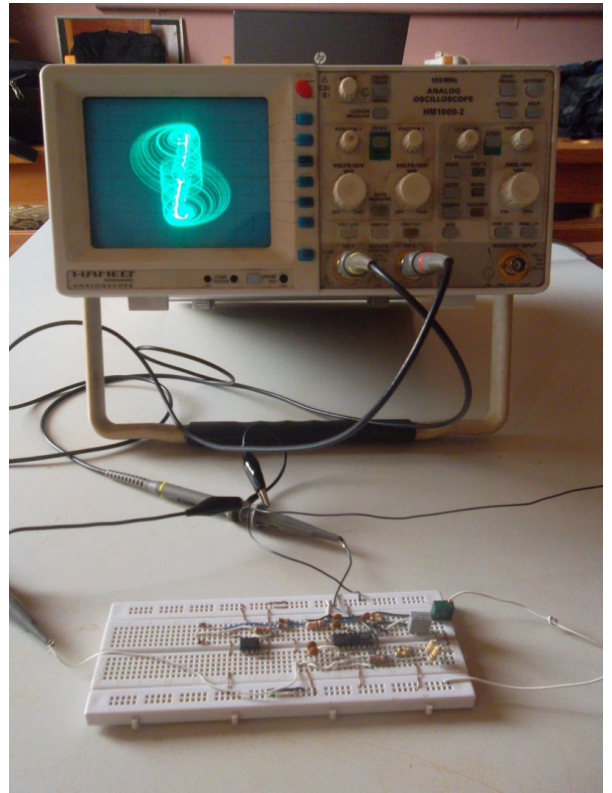
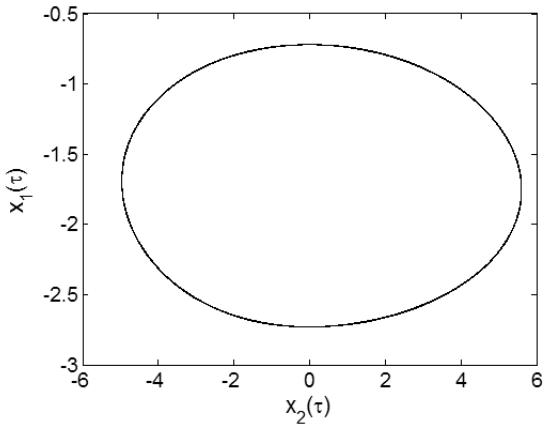
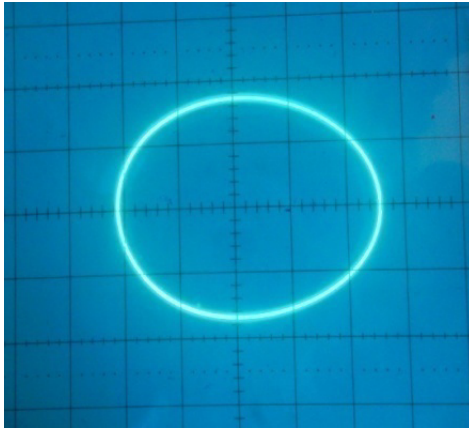


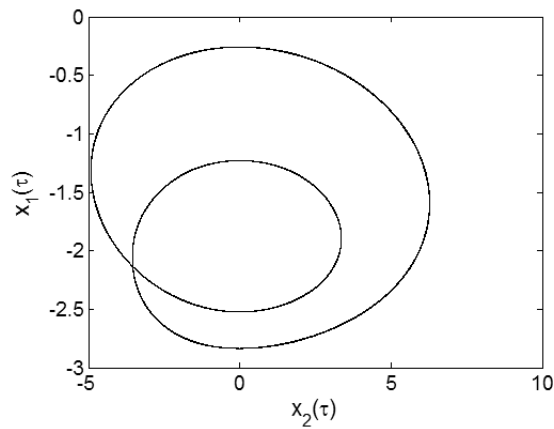
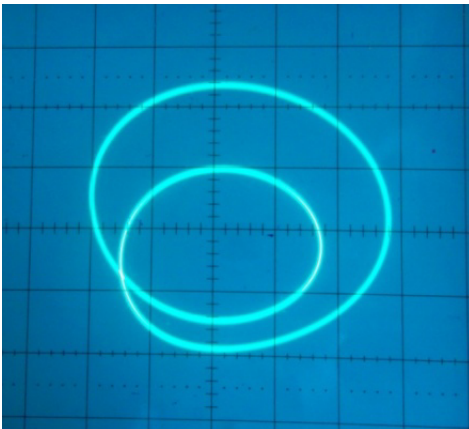
Fig. 11. The experimental jerk circuit in operation. The oscilloscope displays the double-band chaotic attractor captured from the experimental circuit mounted on a breadboard.

attractor \rightarrow double-band chaotic attractor. Some windows of periodic behaviors sandwiched within the chaotic domains are also noted. This is clearly illustrated by the experimental pictures in Fig. 12 showing the real behavior of the jerk circuit under consideration. In light of the pictures in Fig. 12, it can be seen that the real circuit demonstrates the same bifurcation sequences as observed during the numerical study.

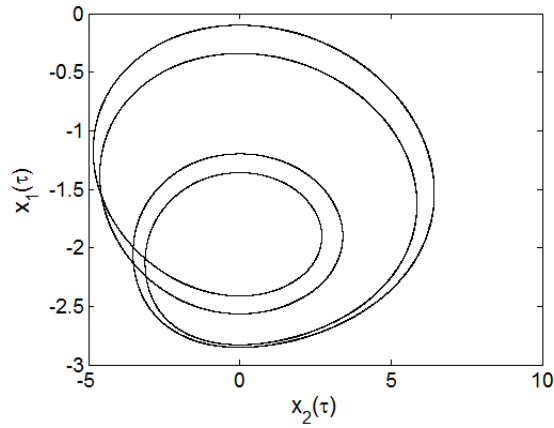
To experimentally provide evidence of coexisting multiple attractors in the jerk circuit, the control resistors are fixed as follows: $R_1 = 25\text{ k}\Omega$; $R_2 = 5.8\text{ k}\Omega$. When switching on and off the power supply (and thereby randomly selecting initial states), either a regular period-4 limit cycle or a single-band chaotic one can be obtained. It should be mentioned that chaotic attractors, with relatively larger basin, are more likely to appear (i.e. more frequent) than periodic ones. Moreover, as expected (owing to the fractal structure of basin boundaries), jumps between coexisting attractors are also observed in experiment. A comparison between experimental and numerical results related to the presence of four



(a)



(b)



(c)

Fig. 12. (Right) Experimental phase portraits obtained from the circuit (with $R_1 = 25 \text{ k}\Omega$) using a dual trace oscilloscope in the XY mode; the corresponding numerical phase portraits are shown on the left. Output voltages X_2 and X_1 are fed to the X and Y inputs respectively: (a) period-1 for $R_2 = 3.6 \text{ k}\Omega$; (b) period-2 for $R_2 = 4.65 \text{ k}\Omega$; (c) period-4 for $R_2 = 5.170 \text{ k}\Omega$; (d) single-band chaos for $R_2 = 5.8 \text{ k}\Omega$; (e) single-band chaos for $R_2 = 8.0 \text{ k}\Omega$; (f) double-band chaos $R_2 = 11 \text{ k}\Omega$. The scales are $X = 2 \text{ V}/\text{div}$ and $Y = 0.5 \text{ V}/\text{div}$ for all pictures except for (f) where the scales are $X = 2 \text{ V}/\text{div}$, $Y = 1 \text{ V}/\text{div}$.

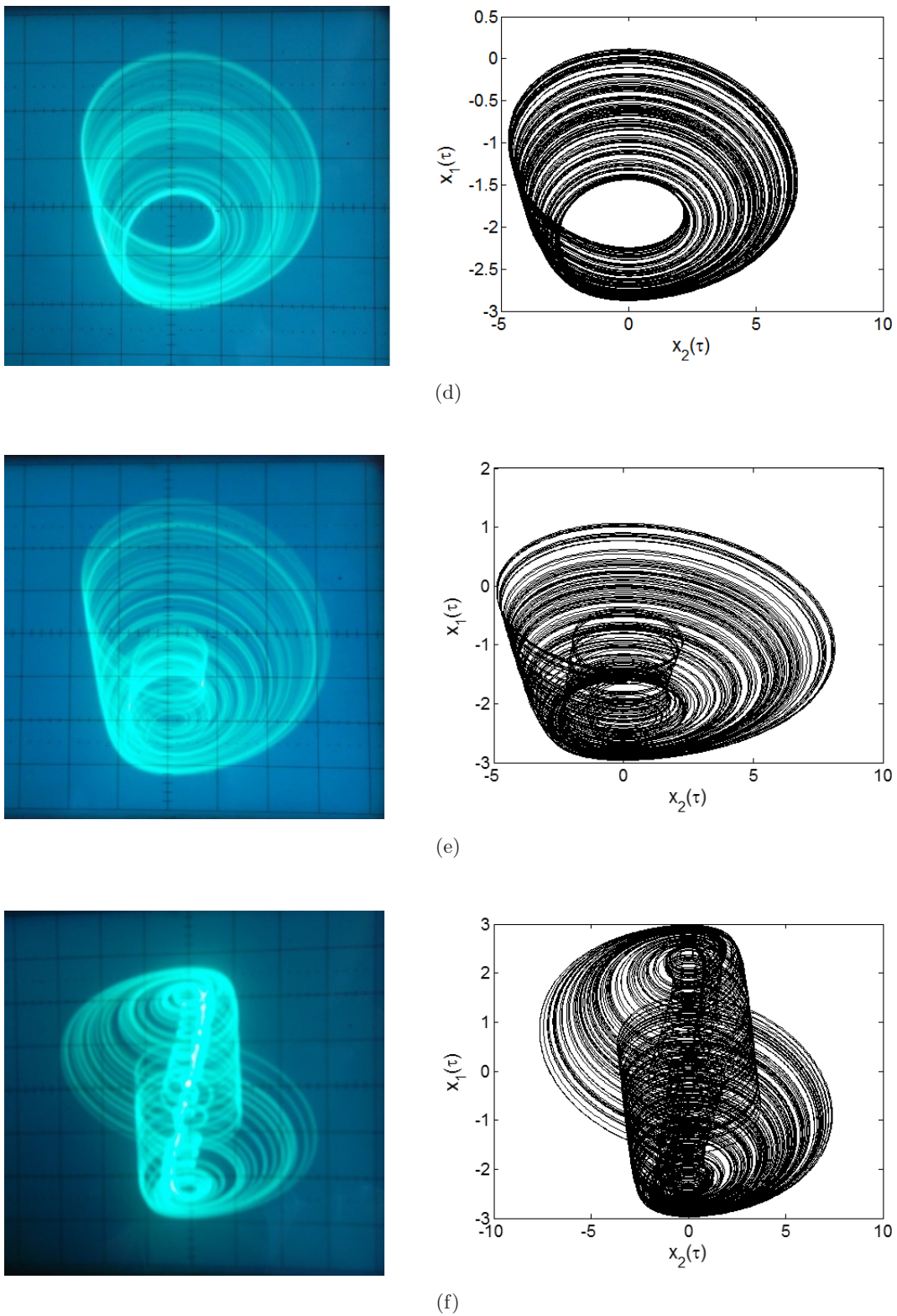


Fig. 12. (Continued)

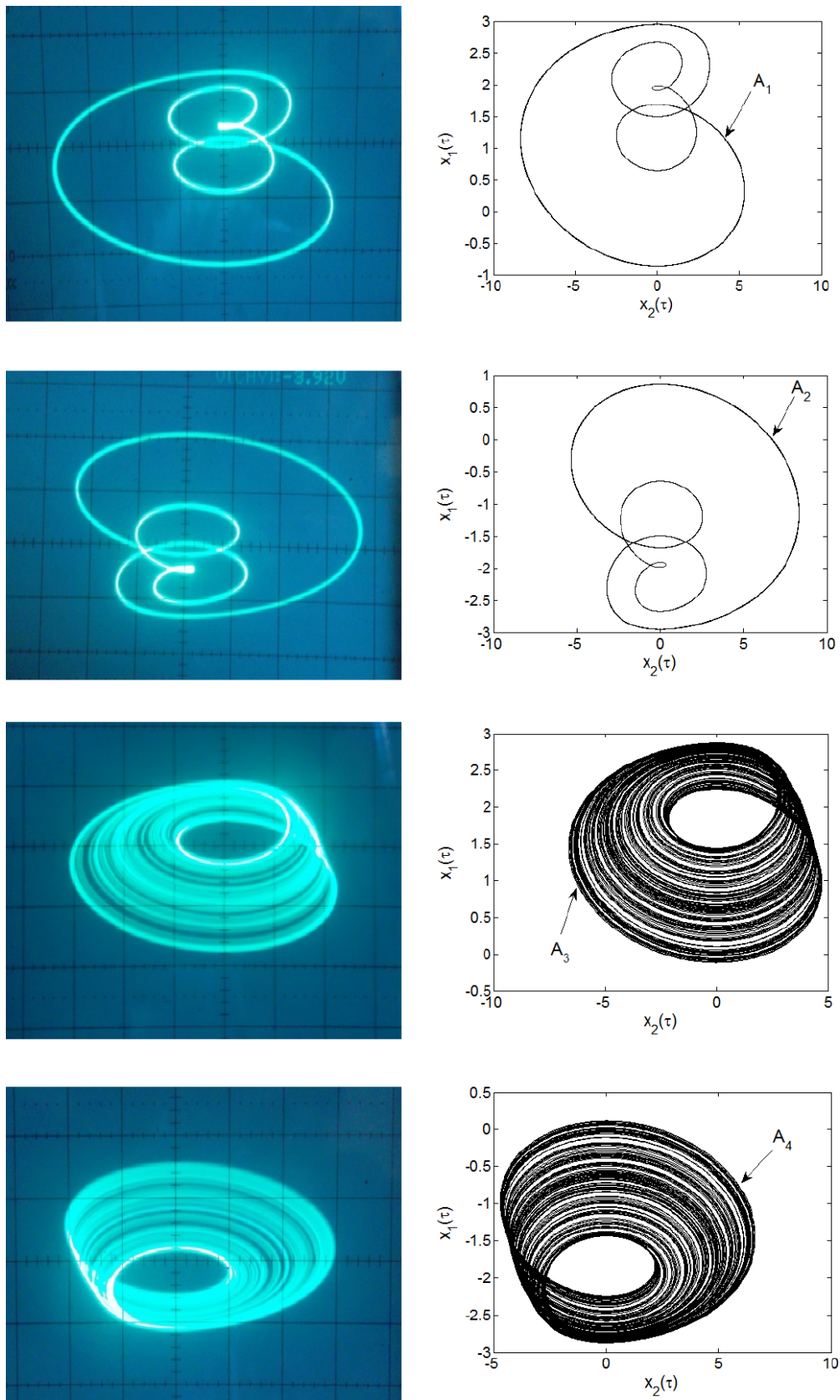


Fig. 13. Coexistence of multiple solutions for $R_2 = 5.8 \text{ k}\Omega$. Both periodic and chaotic attractors appear randomly in the experiment when switching on and off the power supply. The scales are $X = 2 \text{ V/div}$ and $Y = 1 \text{ V/div}$ for all pictures. Note the similarity of those pictures with the numerically obtained ones.

coexisting attractors is presented in Fig. 13. More interestingly, the hysteretic behavior is observed in the experimental jerk circuit by increasing the value of R_2 in such a way that the circuit moves from the state of period-1 motion to develop a double-band chaotic attractor and then decreasing the value of the same resistor to move back to the state of period-1 motion. Thus the system follows a different path while R_2 is decreased rather than R_2 is increased, reminiscent of a hysteresis. Once more a very good qualitative agreement can be captured between numerical and experimental results. However, a slight discrepancy that may be attributed to the precision on the values of electronic components as well as the simplifying assumptions considered during the modeling process (i.e. ideal diode model, ideal op. amplifier) can be noted between numerical and experimental results (see caption in Fig. 12).

Similarly, we have also verified the dynamical behaviors, the transitions from period-doubling bifurcation (period-1, period-2, period-4, period-8 and periodic windows) to chaos, the symmetry recovering crisis, and the coexistence of multiple attractors in the (X_2, X_1) plane evaluated through Pspice simulation, keeping $R_1 = 25\text{ k}\Omega$ and varying the values of resistances R_2 . For instance, using the same parameters set above, we have observed a pair of coexisting chaotic attractors with a pair of coexisting limit cycles when initial capacitors' voltages ($v_{C_1}(0), v_{C_2}(0), v_{C_3}(0)$) were fixed to $(0V, 0V, \pm 0.1V)$ and $(0V, 0V, \pm 1V)$ respectively. However, we have avoided the inclusion of the simulation results for the sake of brevity.

5. Concluding Remarks

This paper has considered the dynamics of a novel jerk circuit which can be regarded as an electronic circuit implementation (i.e. analog simulator) of a linear transformation of Model MO15 introduced in [Sprott, 2010]. Using standard nonlinear analysis techniques such as bifurcation diagrams, Lyapunov exponent plots, time series, Poincaré sections, and frequency spectra, the dynamics of the system has been characterized in terms of its parameters. The bifurcation analysis suggests that chaos arises in the novel jerk circuit following the classical period-doubling and symmetry recovering crises events when adjusting the bifurcation control parameters in small steps. As a major result, it is found that the proposed jerk circuit exhibits

the unusual and striking feature of multiple attractors (i.e. coexistence of four disconnected nonstatic attractors depending solely on initial conditions) for a wide range of circuit parameters. The proposed circuit uses only off-the-shelf electronic components and can be rescaled over a wide range of frequencies. To the best of the authors' knowledge, the jerk circuit introduced in this work represents the simplest electrical circuit (no analog multiplier is needed) reported to date, capable of displaying such type of behavior [Kengne *et al.*, 2016; Rosalie & Letellier, 2013, 2015; Li *et al.*, 2015b; Li & Sprott, 2013a]. Results of theoretical analyses are perfectly traced by laboratory experimental measurements.

An interesting issue under investigation is that of developing some synchronization strategies for the jerk circuit considered in this work owing to potential technological applications (e.g. chaos-based communication, image encryption, random bit generation and so on). Moreover, a detailed exploration of the parameter space (both theoretically and experimentally) with the aim of revealing all regions in which the phenomenon of coexistence of multiple attractors occurs deserves further studies.

References

- Argyris, J., Faust, G. & Haase, M. [1994] *An Exploration of Chaos* (North-Holland, Amsterdam).
- Buscarino, A., Fortuna, L., Frasca, M. & Gambuzza, L. V. [2012] "A chaotic circuit based on Hewlett-Packard memristor," *Chaos* **22**, 023136.
- Cushing, J. M., Henson, S. M. & Blackburn, C. C. [2007] "Multiple mixed attractors in a competition model," *J. Biol. Dyn.* **1**, 347–362.
- Eichhorn, R., Linz, S. J. & Hanggi, P. [2002] "Simple polynomial classes of chaotic jerky dynamics," *Chaos Solit. Fract.* **13**, 1–15.
- Hanias, M. P., Giannaris, G. & Spyridakis, A. R. [2006] "Time series analysis in chaotic diode resonator circuit," *Chaos Solit. Fract.* **27**, 569.
- Hens, C., Dana, S. K. & Feudel, U. [2015] "Extreme multistability: Attractors manipulation and robustness," *Chaos* **25**, 053112.
- Kengne, J., Chedjou, J. C., FonzinFozin, T., Kyamakya, K. & Kenne, G. [2014] "On the analysis of semiconductor diode based chaotic and hyperchaotic chaotic generators — A case study," *Nonlin. Dyn.* **77**, 373–386.
- Kengne, J. [2015] "Coexistence of chaos with hyperchaos, period-3 doubling bifurcation, and transient chaos in the hyperchaotic oscillator with gyrators," *Int. J. Bifurcation and Chaos* **25**, 1550052-1–17.

- Kengne, J., Njitacke, Z. T. & Fotsin, H. B. [2016] "Dynamical analysis of a simple autonomous jerk system with multiple attractors," *Nonlin. Dyn.* **83**, 751–765.
- Kiers, K. & Schmidt, D. [2004] "Precision measurement of a simple chaotic circuit," *Am. J. Phys.* **76**, 503–509.
- Kingni, S. T., Keuninckx, L., Woaf, P., van der Sande, G. & Danckaert, J. [2013] "Dissipative chaos, Shilnikov chaos and bursting oscillations in a three-dimensional autonomous system: Theory and electronic implementation," *Nonlin. Dyn.* **73**, 1111–1123.
- Kingni, S. T., Jafari, S., Simo, H. & Woaf, P. [2014] "Three-dimensional chaotic autonomous system with only one stable equilibrium: Analysis, circuit design, parameter estimation, control, synchronization and its fractional-order form," *Eur. Phys. J. Plus* **129**, 76.
- Kuznetsov, A. P., Kuznetsov, S. P., Mosekilde, E. & Stankevich, N. V. [2015] "Co-existing hidden attractors in a radio-physical oscillator," *J. Phys. A: Math. Theor.* **48**, 125101.
- Leipnik, R. B. & Newton, T. A. [1981] "Double strange attractors in rigid body motion with linear feedback control," *Phys. Lett. A* **86**, 63–87.
- Leonov, G. A. & Kuznetsov, N. V. [2013] "Hidden attractors in dynamical systems. From hidden oscillations in Hilbert–Kolmogorov, Aizerman, and Kalman problems to hidden chaotic attractor in Chua circuits," *Int. J. Bifurcation and Chaos* **23**, 1330002-1–69.
- Leonov, G. A., Kuznetsov, N. V. & Mokaev, T. N. [2015] "Homoclinic orbits, and self-excited and hidden attractors in a Lorenz-like system describing convective fluid motion," *Eur. Phys. J. Special Topics* **224**, 1421–1458.
- Li, C. & Sprott, J. C. [2013a] "Multistability in a butterfly flow," *Int. J. Bifurcation and Chaos* **23**, 1350199.
- Li, C. & Sprott, J. C. [2013b] "Amplitude control approach for chaotic signals," *Nonlin. Dyn.* **73**, 1335–1341.
- Li, C. & Sprott, J. C. [2014] "Coexisting hidden attractors in a 4-D simplified Lorenz system," *Int. J. Bifurcation and Chaos* **24**, 1450034-1–12.
- Li, C., Hu, W., Sprott, J. C. & Wang, X. [2015a] "Multistability in symmetric chaotic systems," *Eur. Phys. J. Special Topics* **224**, 1493–1506.
- Li, C., Sprott, J. C., Yuan, Z. & Li, H. [2015b] "Constructing chaotic systems with total amplitude control," *Int. J. Bifurcation and Chaos* **25**, 1530025-1–14.
- Louodop, P., Kountchou, M., Fotsin, H. & Bowong, S. [2014] "Practical finite-time synchronization of jerk systems: Theory and experiment," *Nonlin. Dyn.* **78**, 597–607.
- Luo, X. & Small, M. [2007] "On a dynamical system with multiple chaotic attractors," *Int. J. Bifurcation and Chaos* **17**, 3235–3251.
- Maggio, G. M., De Feo, O. & Kennedy, M. P. [1999] "Nonlinear analysis of the Colpitts oscillator and application to design," *IEEE Trans. Circuits Syst.-I: Fund. Th. Appl.* **46**, 1118–1130.
- Malasoma, J. M. [2000] "What is the simplest dissipative chaotic jerk equation which is parity invariant?" *Phys. Lett. A* **264**, 383–389.
- Masoller, C. [1994] "Coexistence of attractors in a laser diode with optical feedback from a large external cavity," *Phys. Rev. A* **50**, 2569–2578.
- Massoudi, A., Mahjani, M. G. & Jafarian, M. [2010] "Multiple attractors in Koper–Gaspard model of electrochemical," *J. Electroanalyt. Chem.* **647**, 74–86.
- Nayfeh, A. H. & Balachandran, B. [1995] *Applied Nonlinear Dynamics: Analytical, Computational and Experimental Methods* (John Wiley & Sons, NY).
- Pisarchik, A. N. & Feudel, U. [2014] "Control of multistability," *Phys. Rep.* **540**, 167–218.
- Pivka, L., Wu, C. W. & Huang, A. [1994] "Chua's oscillator: A compendium of chaotic phenomena," *J. Franklin Instit.* **331B**, 705–741.
- Rosalie, M. & Letellier, C. [2013] "Systematic template extraction from chaotic attractors: I. Genus-one attractors with inversion symmetry," *J. Phys. A: Math. Theor.* **46**, 375101.
- Rosalie, M. & Letellier, C. [2015] "Systematic template extraction from chaotic attractors: II. Genus-one attractors with unimodal folding mechanisms," *J. Phys. A: Math. Theor.* **48**, 235100.
- Sprott, J. C. [1997a] "Some simple jerk functions," *Am. J. Phys.* **65**, 537–543.
- Sprott, J. C. [1997b] "Simplest dissipative chaotic flow," *Phys. Lett. A* **228**, 271–274.
- Sprott, J. C. [2000] "Simple chaotic systems and circuits," *Am. J. Phys.* **68**, 758–763.
- Sprott, J. C. [2010] *Elegant Chaos: Algebraically Simple Flow* (World Scientific, Singapore).
- Sprott, J. C. [2011] "A new chaotic jerk circuit," *IEEE Trans. Circuits Syst.-II: Exp. Briefs* **58**, 240–243.
- Strogatz, S. H. [1994] *Nonlinear Dynamics and Chaos* (Addison-Wesley, Reading, MA).
- Sukov, D. W., Bleich, M. E., Gauthier, J. & Socolar, J. E. S. [1997] "Controlling chaos in a fast diode resonator using extended time-delay autosynchronization: Experimental observations and theoretical analysis," *Chaos* **7**, 560–576.
- Swathy, P. S. & Thamilmaran, K. [2013] "An experimental study on SC-CNN based canonical Chua's circuit," *Nonlin. Dyn.* **71**, 505–514.

- Upadhyay, R. K. [2003] "Multiple attractors and crisis route to chaos in a model of food-chain," *Chaos Solit. Fract.* **16**, 737–747.
- Vaithianathan, V. & Veijun, J. [1999] "Coexistence of four different attractors in a fundamental power system model," *IEEE Trans. Circuits Syst.-I* **46**, 405–409.
- Wolf, A., Swift, J. B., Swinney, H. L. & Wastano, J. A. [1985] "Determining Lyapunov exponents from time series," *Physica D* **16**, 285–317.